

Computational Anatomy in the Study of Bone Structure

Julio Carballido-Gamio · Daniel P. Nicoletta

Published online: 31 May 2013
© Springer Science+Business Media New York 2013

Abstract Osteoporosis is a major public health threat for millions of Americans with billions of dollars per year of national direct costs for osteoporotic fractures. Osteoporosis results in a decrease in overall bone mass and subsequent increase in the risk of bone fracture. Bone strength arises from the combination of bone size and shape, the distribution of bone mass throughout the structure, and the quality of the bone material. Advances in medical imaging have enabled a comprehensive assessment of bone structure through the analysis of high-resolution scans of relevant anatomical sites, eg, the proximal femur. However, conventional imaging analysis techniques use predefined regions of interest that do not take full advantage of such scans. Recently, computational anatomy, a set of imaging-based analysis algorithms, has emerged as a promising technique in studies of osteoporosis. Computational anatomy enables analyses that are not biased to one particular region and provide a more complete assessment of the whole structure. In this article, we review studies that have used computational anatomy to investigate the structure of the proximal femur in relation to age, fracture, osteoporotic treatment, and spaceflight effects.

Keywords Statistical parametric mapping (SPM) · Voxel-based morphometry (VBM) · Tensor-based morphometry (TBM) · Statistical shape and density modeling (SSDM) · Bone · Fracture · Aging · Treatment · Fracture risk · Dual x-ray absorptiometry (DXA) · Quantitative computed tomography (QCT) · Magnetic resonance imaging (MRI)

J. Carballido-Gamio (✉)
Department of Radiology and Biomedical Imaging, University of California, San Francisco, 185 Berry St, Suite 350,
San Francisco, CA 94107, USA
e-mail: Julio.Carballido-Gamio@ucsf.edu

D. P. Nicoletta
Musculoskeletal Biomechanics Section, Southwest Research Institute, San Antonio, TX 78238, USA

Introduction

Osteoporosis is characterized by loss of bone mass, structural deterioration, and diminished mechanical properties that compromise bone strength predisposing a person to an increased risk of fracture [1]. Bone strength is a consequence of bone density and bone quality, with bone quality including factors such as trabecular and cortical architecture, bone turnover, mineralization, and cellularity. Although osteoporosis affects most of the bones in the human body, osteoporosis-related fractures of the proximal femur are the most devastating outcome of the disease, often signaling an end to independent living in the functional elderly. A hip fracture usually requires hospitalization and major surgery and is associated with significantly increased morbidity and mortality [2, 3].

Dual x-ray absorptiometry (DXA) is the standard imaging modality for the diagnosis of osteoporosis, assessment of a patient's risk of sustaining an osteoporotic bone fracture, and monitoring response to osteoporosis treatment [4, 5]. DXA provides a 2-dimensional (2D) projection of the scanned region enabling the quantification of areal bone mineral density (aBMD) and 2D geometric measurements of the bone structure. DXA is a low radiation dose imaging technique that is widely available, however, DXA provides 2D measurements of 3-dimensional (3D) structures, and does not capture all factors contributing to bone strength [6].

Quantitative computed tomography (QCT) is the leading 3D imaging modality for the study of osteoporosis. QCT enables the accurate quantification of 3D bone geometry, and the accurate estimation of volumetric bone mineral density (vBMD), which is an important surrogate of bone strength [7]. QCT also enables the application of finite element modeling (FEM), which is a numerical engineering technique that enables the prediction of the performance of a structure when subjected to an external load. QCT-based FEM estimates bone strength based on bone geometry, distribution of material properties derived from vBMD values, and clinically relevant loading conditions such as single-limb stance or a fall to the

side with an impact on the posterolateral or lateral aspect of the greater trochanter [8, 9]. Recently, QCT has also been used for the accurate quantification of cortical bone thickness [10]. However, QCT cannot provide high-spatial resolution images to quantify the trabecular bone microstructure due to the high radiation dose that would be needed to achieve the required spatial resolution [11].

Recent advances in hardware, pulse sequence development, and coil design have allowed magnetic resonance imaging (MRI) to be used as an additional alternative to the study of osteoporosis in relevant sites such as the proximal femur [12, 13]. While MRI cannot provide measures of bone density, MRI enables the quantification of bone geometry and the acquisition of high-spatial resolution images for the quantification of trabecular bone microstructure [11]. Recent studies have also shown the feasibility of micro-FEM analysis and cortical bone thickness quantification using MRI [14–16]. Furthermore, MRI goes beyond structural measures by enabling the generation of accurate bone maps of the distribution of marrow-fat fraction [17].

Conventional image analysis approaches are based on predefined regions of interest averaging tissue features over those regions, thus obscuring local information regarding the distribution of the features and how such 2D/3D features contribute to the integrity of the investigated tissue. In contrast, computational anatomy techniques are not biased to one particular region and give an even-handed and comprehensive assessment of parametric differences throughout the structure of interest. Computational anatomy algorithms, initially developed for brain imaging analysis where they have shown their significant potential, have been slowly, but successfully, integrated into studies of osteoporosis.

In this article, we provide an overview of studies that have used computational anatomy in the context of osteoporosis. We start by briefly introducing the basic principles that are needed to understand the concept of computational anatomy. Then for each imaging modality, namely DXA, radiography, QCT, and MRI, we present a summary of studies that have used computational anatomy to investigate the structure of the proximal femur in relation to hip fracture risk, osteoporosis treatment, age, and/or spaceflight effects. We have selected the proximal femur because it is by far the anatomical site that has been most studied with computational anatomy algorithms and because its relevance in osteoporosis. We conclude the article with a brief discussion of the future work in the field of computational anatomy and osteoporosis.

Computational Anatomy

Computational Anatomy is a set of imaging analysis techniques that model anatomical structures in images as curves, surfaces, maps, and volumes with the objective of combining

them across subjects to create statistical feature maps. The statistics of features can then be spatially analyzed based on information from several subjects to detect subtle changes that are associated with prognosis, progression, treatment, or other variables of interest, making it possible to visualize group differences or longitudinal changes as statistical maps [18].

The first step in the conventional approach of computational anatomy requires the spatial normalization of the individual feature maps. Spatial normalization refers to the process of removing, to the extent possible, the natural anatomical variability in a population by deforming each individual's anatomy into a standardized space [19]. After spatial normalization, feature maps can be compared locally and comparisons can be interpreted as being done at corresponding anatomic locations.

Spatial normalization is commonly accomplished in 3 steps: (1) selection of the standardized space, (2) alignment of all the scans in the study to the standardized space using an affine transformation to correct for translation, rotation, and size, and (3) nonlinear registration of the affine registered scans to accommodate for the remaining anatomical variability. Usually the second and third steps are concatenated into a single step.

After spatial normalization, statistical tests are usually performed on a voxel-by-voxel basis (3D; pixel-by-pixel in 2D) generating statistical maps, and P-values are corrected for multiple comparisons to identify regions where the feature of interest is significantly related with the effect of interest.

Other approaches, specifically those that include studying variations in shape, take a slightly different approach based on active shape modeling [20]. In this method, the parameter space is defined by mapping a dense set of surface points onto each individual anatomical structure. The surface points are then optimally repositioned to ensure point-to-point correspondence across the population of interest such that each point on each individual structure corresponds to the same anatomical location. In these approaches, principal component analysis (PCA) is applied to the aligned shapes and/or corresponding volumetric data and the association of the calculated principal components and the effect of interest is investigated.

DXA – Radiography

In this section we discuss early and recent 2D applications of computational anatomy to study the structure of the proximal femur in relation to hip fracture risk using shape and/or intensity features.

Hip Fracture Risk

Gregory and colleagues perform pioneering work in the study of the relationship between the shape of the proximal

femur and osteoporotic hip fractures [21]. The authors studied 26 women who had sustained hip fracture (mean age = 69.2 ± 6.3 years), and 24 gender- and age-matched controls (mean age = 69.1 ± 6.5 years). An active shape model (ASM) of the proximal femur was generated, and using stepwise linear discriminant analysis on the principal modes of shape variation, the probability that a given subject would belong to the fracture group was estimated and referred as PShape. Linear discriminant analysis was used to assess the strength of PShape, DXA-aBMD, and PShape combined with DXA-aBMD to discriminate between the groups. Results showed that by adding ASM features to the Ward's triangle aBMD improved the accuracy of the fracture discrimination from 82 % to 90 %. This work also demonstrated that ASM features were independent of age, body mass index, and aBMD. A year later Gregory and colleagues perform a similar study on the same dataset where they showed that the addition of trabecular structural measures to DXA-aBMD and ASM features improved the discrimination between fracture cases and controls with an area under the receiver operator characteristic (ROC) curve (Az) reaching a value of 0.99 [22].

Baker-LePain and colleagues applied active shape modeling to a nested-control study of incident hip fracture in white women [23]. The study included radiographs of the proximal femur of 168 women with incident hip fracture (mean age = 71.7 ± 4.6 years) and 231 controls (mean age = 70.6 ± 4.4 years). The association of ASM modes of the proximal femur with incident hip fracture was investigated using logistic regression. In models controlling for age and body mass index, Az for hip shape was 0.813, and it improved when ASM modes were combined with femoral neck DXA-aBMD to 0.835.

Following the work of Gregory and colleagues [21, 22], Goodyear used DXA of the proximal femur in a prospective study of incident hip fracture that included 182 women with incident hip fracture (mean age = 81.5 ± 4.6 years) and 364 gender-, age-, weight-, and height-matched controls (mean age = 81.5 ± 4.5 years) [24]. The authors generated an ASM and an active appearance model (AAM; shape and patterns of aBMD), and used logistic regression to evaluate the association between incident hip fracture with DXA-aBMD, shape modes, and appearance modes. ROC analysis showed that the combination of the second shape mode, the sixth appearance mode, and aBMD improved the prediction of hip fracture by 3 % compared with any single predictor, and demonstrated that the shape and appearance modes used in the prediction model were independent predictors of hip fracture after adjusting for aBMD. According to the authors, this slight improvement represents the prediction of additional 2000 and 10000 hip fracture cases per year in the UK and US, respectively.

QCT

In this section we present QCT studies that have used vBMD, cortical bone thickness, FEM, and shape as features for the ex-vivo and in-vivo study of bone structure using computational anatomy.

Spaceflight Effects

Li and colleagues presented the first 3D application of computational anatomy for the study of bone structure [25]. The authors studied the effects of spaceflight on the proximal femur of 16 astronauts (mean age 44.6 ± 4.0 years) during spaceflight durations of 4–6 months on the International Space Station. QCT scans were obtained before (30–60 days prior to launch) and after spaceflight (7–10 days of landing). All QCT scans were spatially normalized to a common reference to create pre-flight and post-flight composite hip models of vBMD, which enabled the visualization of the distribution of gradients of bone loss. The authors then performed paired t-tests on a voxel-by-voxel basis, and used false discovery rate (FDR) correction to correct for multiple comparisons, yielding maps indicating regions inside the proximal femur with significant bone loss. These maps indicated that the superior aspect of the femoral head experienced greater bone loss than other regions of the proximal femur. The authors hypothesized that these results could be due to focal bone loss in the principal compressive band of trabeculae, the medial aspect of which is located in the femoral head. In prolonged mechanical unloading situations such as a spaceflight, the largest bone losses are known to occur in those regions that are most heavily used in normal usage, and the principal compressive band is 1 of the major load-bearing structures in the hip.

Hip Fracture Risk

A year later, Li and colleagues applied their statistical parametric mapping (SPM) technique of the spaceflight study to a cross-sectional study of hip fracture in Chinese women [26]. QCT scans of 37 women (65 years old or older) with hip fracture, and 38 gender- and age-matched controls were registered to a common reference space to create a voxel-based statistical atlas of vBMD. The authors then used this atlas to perform t-tests between the 2 groups on a voxel-by-voxel basis correcting for multiple comparisons with FDR, and identified regions inside the proximal femur where vBMD was significantly associated with hip fracture. Three main clusters were identified, 1 in the femoral head, 1 in the femoral neck, and a third one in the trochanteric region. The clusters in the femoral neck and trochanter agreed with previous studies in the literature indicating that these 2 locations are commonly involved in hip fracture.

The finding in the femoral head, suggested that this commonly ignored region, could play a significant role in the study of hip fracture. In the same study, fracture discrimination was assessed using mean vBMD values from the conventional volumes of interest and the 3 identified clusters, showing that fracture discrimination could be improved by focusing on vBMD values of the fracture-critical regions. The authors also reported that women with neck fracture had lower vBMD in a small region near the femoral neck and the femoral head ($P=0.014$), and women with trochanteric fracture had lower vBMD in trochanteric regions such as the internal calcar septum ($P=0.006$).

Poole and colleagues applied SPM of cortical bone thickness to identify focal osteoporosis in a cross-sectional study of hip fracture [27]. They studied 150 women, 75 with acute fracture, and 75 age-matched controls (mean age = 76.6 ± 7.3 years). Thirty-six women had femoral neck fracture (mean age = 78.1 ± 7.1 years), and 39 trochanteric fracture (mean age = 75.2 ± 7.9 years). Surface maps of cortical bone thickness were calculated for each subject based on QCT scans [10], and spatially normalized to a common frame of reference. The authors then investigated differences in cortical thickness between: (1) femoral neck fracture cases ($n=36$) and controls ($n=75$), and (2) trochanteric fracture cases ($n=39$) and controls ($n=75$). The authors fitted a model to the statistical atlases where the model effects were group, age, height, and weight. T-statistics were calculated to test the significance of the group term, and random field theory was used to correct for multiple comparisons. Significant focal cortical thinning was observed in women with hip fracture compared with controls. Cortical thinning was observed in different regions in women with neck fracture compared with women with trochanteric fracture. The largest region of cortical thinning was the head-neck junction showing a thumbnail-size patch of up 30 % of cortical thinning in neck fracture cases. This region is commonly involved in hip fracture. Other regions included patches in the greater and lesser trochanter for both types of fracture. No regions of statistically significant thicker bone were observed in fracture cases.

Recently, Carballido-Gamio and colleagues applied SPM, specifically voxel-based morphometry (VBM), to a prospective study to identify regions inside the proximal femur where vBMD was significantly associated with incident hip fracture [28, 29••]. They studied 222 women from a population-based cohort of Icelandic women, 74 with incident hip fracture (mean age = 79.4 ± 5.9 years) and 148 without fracture (mean age = 79.2 ± 5.7 years). QCT scans of the proximal femur were acquired at baseline (before hip fracture), and spatially normalized to a common reference to generate a statistical atlas of vBMD. The authors then fitted a general linear model on a voxel-by-voxel basis to generate a Student's t-test statistical map of the voxelwise vBMD differences between controls and fracture cases. The vBMD values were used as the dependent

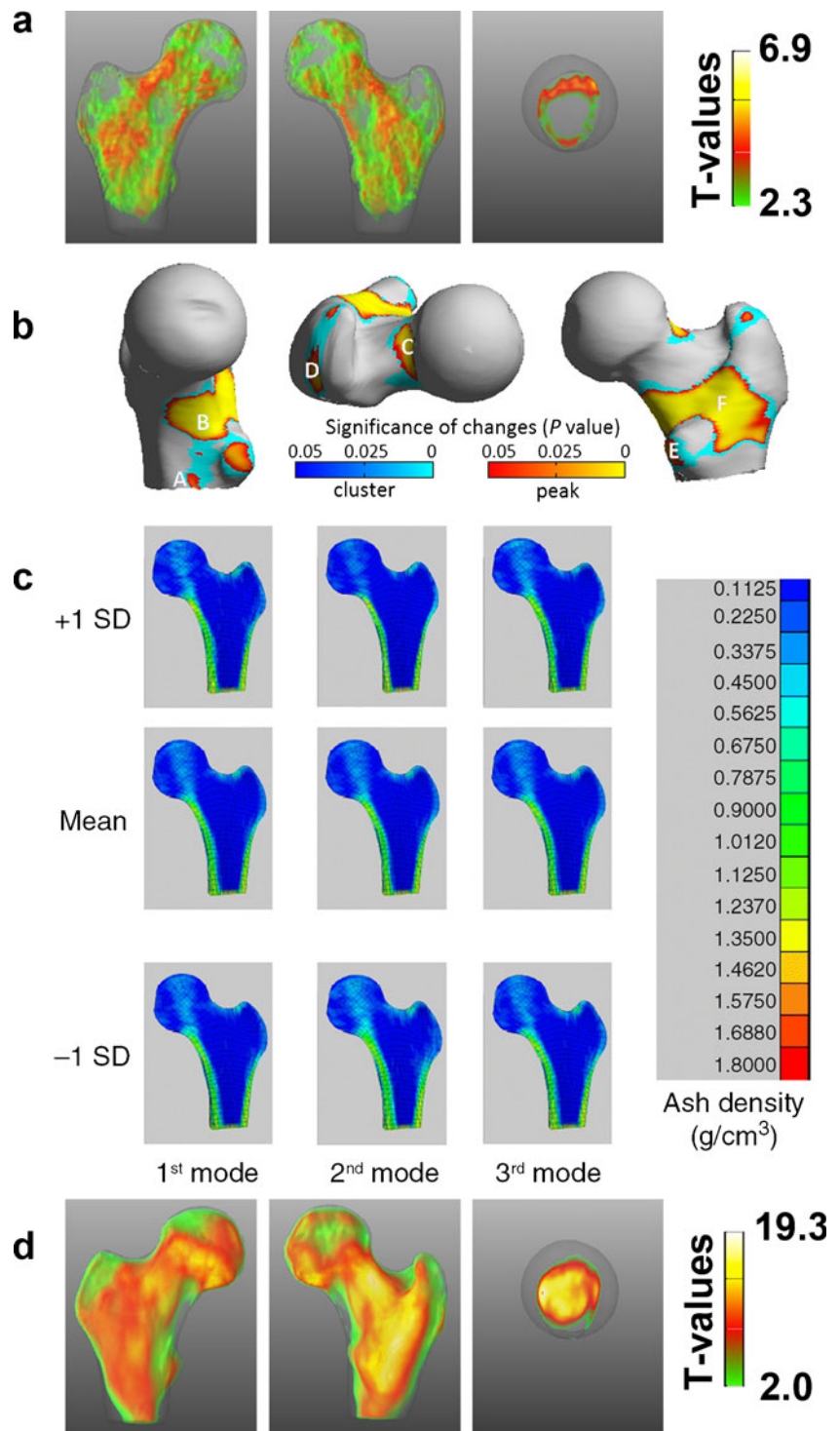
variable, and group membership as the independent variable (controls or fracture). Age, height, and weight were incorporated as covariates, and FDR was used to correct for multiple comparisons. Results indicated significant bone loss in fracture cases compared with controls in regions commonly involved with hip fracture, namely the neck and trochanteric regions. However, the authors also reported significant bone loss in fracture cases at the inferomedial proximal femoral cortex (Fig. 1a), a primary load-bearing region that in an aging study performed in parallel by the same authors [29••], showed minimal differences between young and older American women.

In the same population-based cohort of Icelandic women (74 with incident hip fracture and 148 without fracture), Carballido-Gamio and colleagues studied the local association of shape with incident hip fracture in the proximal femur [28] using tensor-based morphometry (TBM) [30]. TBM processes the displacement vectors that are assigned to each voxel during the nonlinear step of spatial normalization, and for each voxel calculates the amount of contraction or expansion that is needed to match the standardized space generating shape feature maps. Contraction-expansion maps were then compared between controls and fracture cases with a similar voxel-wise approach as for vBMD to generate an FDR-corrected Student's t-test statistical map. TBM showed volume loss in the principal compressive bands and cortices, and enlargement of the trabecular neck area in fracture women compared with age-matched controls. A focal region of cortical volume loss in the superior neck of fracture women was also observed in agreement with a previous study indicating cortical thinning in this area [31].

Osteoporosis Treatment

Poole and colleagues published what has been so far the only application of computational anatomy in a study of osteoporosis treatment [32••]. The authors studied a total of 238 femora from 65 women (mean age 67.5 ± 6.8 years) with severe osteoporosis that were treated with recombinant human parathyroid hormone (hPTH-(1–34)) for 24 months. QCT scans of the proximal femur were acquired at baseline and 24 months. The authors generated surface maps of cortical bone thickness [10], and aligned all of them to a common reference frame. Surface maps representing response to treatment were generated for each subject by subtracting the baseline maps from the 24-month maps, and averaging the left and right difference maps when both were available, thus yielding a total of 65 response maps. The authors then fitted a model to the response maps, and used T-statistics and random field theory to correct for multiple comparisons with the aim of detecting regions where hPTH-(1–34) caused a significant positive thickness change. Results indicated significant cortical thickening despite ageing effects in regions of high stress

Fig. 1 (a) Student's *t*-test statistical maps indicating regions where vBMD was significantly associated with incident hip fracture (3D anterior, 3D posterior, and 3D femoral neck cross-sectional views) [29••]. (b) P-value maps indicating regions of significant cortical bone thickening in response to osteoporosis treatment (3D medial, 3D superior, and 3D posterior views) [32••]. (c) Finite element models constructed from a statistical shape density model [35••]. (d) Student's *t*-test statistical maps indicating regions where vBMD was significantly associated with aging (3D anterior, 3D posterior, and 3D femoral neck cross-sectional views) [29••]. In (a) and (d), nonsignificant voxels were rendered transparent



in normal locomotion: (1) inferomedial junction of the cortex with the load-bearing calcar femorale, and (2) the head-neck junction of the superior cortex (Fig. 1b). Both regions are commonly involved in hip fracture. The authors also identified focal thickening at the enthuses of powerful locomotion muscles in the greater (gluteus medius) and lesser trochanter (psoas), and at the inter-trochanteric region (quadratus femoris). No significant cortical thinning was observed. Authors suggested a

possible synergistic effect of habitual load and PTH, since significant cortical thickening was seen at sites that are highly stressed by walking.

FEM

QCT-based FEM provides accurate predictions of bone strength, however, the generation of subject-specific models

is a time consuming and computational intense problem, which has limited this Mechanical Engineering technique to research studies and hampered its translation to the clinic. Even in the research field, population-based studies using FEM is still limited to a reduced number of research centers. For these reasons, efforts are currently in progress to improve the practicality of FEM for the study of bone strength in osteoporosis.

In the work of Bryan and colleagues [33], statistical-deformation models [34] were used to generate a statistical atlas of elastic material properties of the proximal femur. QCT scans of 8 women and 13 men (mean age=68 years; 43–84 years) were used to define point correspondence between scans, and principal component analysis (PCA) was used to summarize the variation in shape and material properties (8 PCA modes). The purpose of the study was then to generate 1000 realistic and unique finite element models to be used on a study of femoral neck fracture risk. Simulations of the impact of an oblique fall to the side on the 1000 models indicated that 28 of the 1000 femora were at high risk of neck fracture. The location more likely to sustain fracture was the intertrochanteric region, and the authors reported that the percentage of cortical bone in the proximal femur was the main differentiator between the failed and non-failed groups.

A more recent work in the field of QCT, FEM, and computational anatomy was published by Nicoletta and Bredbenner [35•]. The objective of their study was to develop a parametric finite element model of the proximal femur and show how this parametric model can be used to reconstruct the 3D shape and bone density distribution of a previously unseen femur. For this purpose, the authors built a statistical shape density model (SSDM; Fig. 1c) using QCT scans of 7 fresh-frozen human female femora (mean age=69.9 ± 8.8 years). Point-to-point correspondence was automatically established on the segmented femora, and PCA was applied to the matched data. For each bone element in the QCT scans, elastic–plastic material behavior with linear hardening was assumed, and isotropic elastic and hardening moduli and ultimate stress values were determined as functions of ash density using empirical relationships [36]. Using a leave-one-out strategy, the authors demonstrated that a 3D finite element model of an unknown femur was reconstructed from the SSDM with an average spatial error of 0.016 mm and an average density error of 0.037 g/cm³. The authors also demonstrated that relatively large differences in predicted bone strength can be observed with relatively subtle changes in bone shape and density distribution. They argue that traditional clinical measures of bone density may not be sensitive enough to detect these relatively minor structural and material variations.

Age

Carballido-Gamio and colleagues performed an aging study [28, 29] in parallel to the incident hip fracture study using

VBM and TBM. The authors studied 349 American women from a population-based cohort (21–97 years), and subdivided them into 3 groups based on their age: (1) young women ($n=94$; mean age=34.1 ± 6.6 years), (2) middle-age women ($n=98$; mean age=51.9 ± 4.0 years), and (3) older women ($n=157$; mean age=72.5 ± 8.8 years). QCT scans were spatially normalized to a common reference to generate vBMD and contraction-expansion statistical atlases. Comparisons of vBMD and contraction-expansion maps were performed on a voxel-by-voxel basis between young and middle-age, and between young and older women. Comparisons were made in the form of general linear models adjusting for weight and height, thus generating Student's t-test statistical maps. P-values were corrected for multiple comparisons using FDR to indicate regions where vBMD or shape was significantly associated with aging. Most of the proximal femoral regions showed significant vBMD loss with aging, with the femoral neck and medial femoral head showing the greatest loss. However, the inferior cortex, a region constantly loaded in daily activities such as walking, indicated preservation of vBMD with aging (Fig. 1d). In terms of shape, TBM showed volume loss in the principal compressive bands and cortices, and enlargement of the trabecular neck area in middle-age and older women compared with young women.

Prediction of Outcome of Interest

As discussed in the previous paragraphs, computational anatomy has been primarily used for the identification of regions or/and features significantly associated with an effect of interest (space flight effects, hip fracture risk, osteoporosis treatment, aging), or as a mean to generate new realistic data (FEM), however, computational anatomy in conjunction with other computational imaging analysis techniques, such as machine learning can be used to predict an outcome of interest.

Li and colleagues had already shown the utility of fracture-critical regions identified by SPM for hip fracture discrimination [26]. Using the same dataset of the hip fracture study of older Chinese women, Li and colleagues built a fracture risk linear model [37]. The population was divided into training and tests sets, and PCA was performed on the spatially normalized training vBMD scans. The principal components that showed a stronger association with hip fracture were selected, and the projections (eigenvalues) of the training scans on these principal components (eigenimages) along with the known fracture status ($Fx_index=0$ for controls and $Fx_index=1$ for fracture) were used to calculate the coefficients of the linear model. The model was then applied to the spatially normalized test vBMD scans to estimate a fracture risk index that was used to discriminate the fracture cases and controls. Results showed comparable

performance to fracture discrimination based on conventional densitometric QCT analysis, however the authors highlighted the potential utility of the principal components as features to be explored in future studies of osteoporosis. Li and colleagues also implemented an image similarity technique to discriminate fracture cases and controls [38]. The same dataset of older Chinese women [26] was subdivided into training and test scans, and the spatially normalized tests scans were classified as either fracture cases or controls based on its vBMD similarity to the spatially normalized training controls and fracture cases. The authors showed that combining vBMD with image similarity measures resulted in improved hip fracture risk estimation.

Fritscher and colleagues used CT statistical models of appearance (shape and spatial intensity distribution) and tested the performance of PCA, independent component analysis, and locally linear embedding (LLE) techniques to generate prediction models of vBMD and break away torque (BT) on predefined regions of interest in the femoral head of 28 femur specimens [39]. Based on the leave-one-out strategy the authors reported that PCA and LLE led to the best results for the prediction of both BT and BMD. The same research group used 100 QCT scans of human cadaver specimens (64 from females with mean age=80.1 ± 9.9 years; and 36 from males with mean age=78.9 ± 11.8 years) to generate a statistical appearance model and evaluate the performance of 5 different regions of interest to predict individual fracture load (FL) [40]. Using principal component regression, leave-one-out tests, and DXA-aBMD as standard of comparison, significant better results for FL prediction were reported using the model-based approach ($R=0.91$) than using DXA-aBMD as predictor ($R=0.81$). The feasibility of applying the work of Fritscher and colleagues [39] on the lumbar spine was shown by Leber and colleagues on a QCT study of 17 spinal specimens [41]. Similarly, Whitmarsh in collaboration with Fritscher and Schubert applied statistical models of appearance and regression models for the assessment of hip fracture risk [42]. They studied 58 women with (mean age=79 ± 10 years) and 58 women without hip fracture (mean age=55 ± 12 years). Using DXA-aBMD from the femoral neck as standard of comparison, and Fisher linear discriminant analysis, the authors showed improved fracture discrimination with the model-based approach (Fisher criterion 6.70 vs 0.98).

In a preliminary investigation [43], Bredbenner and colleagues assessed the ability of SSDM to [35••] discriminate between fracture and non-fracture cases in the Osteoporotic Fractures in Men (MrOS) Study [44]. Baseline QCT data was obtained for 40 randomly selected subjects (20 who subsequently fractured their hip and 20 who did not; age ≥ 65 years) and was processed to develop a parametric

representation of the proximal femur geometry and bone density distribution for each of the 40 subjects [35••]. A parameter vector composed of over 36,000 geometry and bone density variables that correspond between all individuals represented the shape and bone density of each proximal femur. The authors reduced this data set to 39 independent trait combinations variables (TCV) using PCA, where each independent variable consisted of a unique combination of the original 36,000 shape and density parameters. They found that the first 20 TCVs described over 98.0 % of the variability in this set of 40 femurs and 3 TCVs were found to be significantly different between fracture and no fracture groups. The authors stated that these 3 new trait variables describe the independent, complex, and subtle differences in 3D shape and bone density between individuals in the fracture group and no-fracture group. Using a stepwise logistic regression of TCVs against fracture or non-fracture group membership, TCVs appeared to be more successful as a fracture risk discriminator than DXA aBMD measurements alone. A discriminator based on 4 TCVs resulted in as ROC Az of 0.98 compared with an Az of 0.88 using a discriminator based on aBMD alone.

In a later investigation [45], Bredbenner and colleagues applied SSDM methods to a larger sample of 450 men selected from the MrOS study cohort (age ≥ 65). This sample included 40 fracture cases (mean 6.9 year observation, validated by physician review) and 410 non-cases. Using baseline QCT data, SSDM was used to develop an independent set of TCVs of which TCVs 1–11 explained 90 % of the shape and bone density variation and TCVs 1–51 explained 99 % of the shape and bone density distribution variance in this sample. The authors used a step-wise logistic regression to develop fracture classifiers based on SSMD derived TCVs as well as age, BMI, and aBMD from DXA. TCVs were significantly more successful as a fracture risk discriminator than DXA aBMD measurements alone with an ROC Az of 0.9900 for the discriminator constructed using TCVs compared with an Az of 0.8203 using total hip aBMD. When adjusted for age and BMI, the TCV based fracture discriminator resulted in an Az of 0.9951. Furthermore, the authors showed that the TCV-based discriminator correctly classified 8 times as many fracture cases compared with aBMD alone.

Later, Whitmarsh and colleagues took an interesting 2D-3D approach for hip fracture discrimination [46]. The authors constructed a 3D statistical model of appearance based on QCT scans of 180 women (mean age=67.8 ± 17.0 years). The model was then registered to match 2D DXA scans of a fracture and a control group. The fracture group consisted of 175 women (mean age 66.4 ± 9.9 years) who sustained a fracture on the contralateral femur, and the control group of 175 women (mean age=65.3 ± 10.0 years) with no history of fracture. The fracture discrimination ability of the 3D-to-

2D registration parameters and DXA-aBMD was evaluated using logistic regression analysis. Az was 0.802 for DXA-aBMD, and 0.840 for the combination of model parameters with DXA-aBMD showing a slight improvement when the 3D model was used in addition to DXA-aBMD for hip fracture discrimination.

MRI

Up to date, there has been only 1 study that has used computational anatomy in the proximal femur with MRI in the context of osteoporosis. Carballido-Gamio and colleagues generated a shape atlas of the proximal femur and demonstrated its utility for the consistent automatic positioning of regions of interest in conventional region-of-interest-based cross-sectional studies of trabecular bone microstructure [47]. However, the authors also showed that proximal femoral parametric maps of trabecular bone microstructural features can be generated using high-spatial resolution MRI scans, and potentially used for region-of-interest-free analyses.

Conclusions

In this review, we have provided a summary of the most recent work involving computational anatomy for the study of bone structure in osteoporosis, with particular emphasis on the proximal femur. QCT, radiography, and DXA are by far the imaging modalities that have received the greatest amount of attention since, until recently, they were the only clinical imaging techniques capable of the *in vivo* study of deep seated locations like the proximal femur. MRI, which is now also capable of generating high-spatial resolution scans of this anatomic location, could also play a significant role in the field through the generation of accurate fat-fraction maps and the analysis of trabecular bone microstructure. Another imaging modality that could be important in computational anatomy studies of osteoporosis is high-resolution peripheral QCT (HR-pQCT). Although limited to imaging of the extremities (distal radius and distal tibia), HR-pQCT provides the capability of generating maps of vBMD, trabecular bone microstructural parameters, cortical bone thickness, and, when combined with FEM, can be used to predict bone strain and stress. Significant knowledge has been accomplished with conventional region-of-interest-based imaging analysis techniques with respect to bone structure, however, computational anatomy techniques will certainly help to provide a deeper understanding of the structural deterioration and pathophysiological processes that accompany osteoporosis. Furthermore, the combination of computational anatomy with

machine learning approaches will improve the prediction of outcomes of interest such as the risk of hip fracture.

Compliance of Ethics Guidelines

Conflict of Interest J Carballido-Gamio declares that he has no conflicts of interest. DP Nicoletta declares that he has no conflicts of interest.

Human and Animal Rights and Informed Consent This article does not contain any studies with human or animal subjects performed by any of the authors.

References

Papers of particular interest, published recently, have been highlighted as:

•• Of major importance

1. Osteoporosis prevention, diagnosis, and therapy. NIH consensus statement. 2000;17:1–36.
2. Kanis JA, Oden A, Johnell O, et al. The components of excess mortality after hip fracture. *Bone*. 2003;32:468–73.
3. Foss NB, Kehlet H. Mortality analysis in hip fracture patients: implications for design of future outcome trials. *Br J Anaesth*. 2005;94:24–9.
4. Blake GM, Fogelman I. The role of DXA bone density scans in the diagnosis and treatment of osteoporosis. *Postgrad Med J*. 2007;83:509–17.
5. Genant HK, Engelke K, Prevrhal S. Advanced CT bone imaging in osteoporosis. *Rheumatology*. 2008;47 Suppl 4:iv9–iv16.
6. Majumdar S. Magnetic resonance imaging for osteoporosis. *Skeletal Radiol*. 2008;37:95–7.
7. Lang TF. Quantitative computed tomography. *Radiol Clin North Am*. 2010;48:589–600.
8. Keyak JH, Rossi SA, Jones KA, Skinner HB. Prediction of femoral fracture load using automated finite element modeling. *J Biomech*. 1998;31:125–33.
9. Keyak JH, Kaneko TS, Tehranzadeh J, Skinner HB. Predicting proximal femoral strength using structural engineering models. *Clin Orthop Relat R*. 2005;219–28.
10. Treece GM, Gee AH, Mayhew PM, Poole KE. High resolution cortical bone thickness measurement from clinical CT data. *Med Image Anal*. 2010;14:276–90.
11. Carballido-Gamio J, Majumdar S. Clinical utility of microarchitecture measurements of trabecular bone. *Curr Osteoporos Rep*. 2006;4:64–70.
12. Krug R, Banerjee S, Han ET, et al. Feasibility of *in vivo* structural analysis of high-resolution magnetic resonance images of the proximal femur. *Osteoporos Int*. 2005;16:1307–14.
13. Krug R, Burghardt AJ, Majumdar S, Link TM. High-resolution imaging techniques for the assessment of osteoporosis. *Radiol Clin North Am*. 2010;48:601–21.
14. Newitt DC, van Rietbergen B, Majumdar S. Processing and analysis of *in vivo* high-resolution MR images of trabecular bone for longitudinal studies: reproducibility of structural measures and micro-finite element analysis derived mechanical properties. *Osteoporos Int*. 2002;13:278–87.
15. Wehrli FW. Structural and functional assessment of trabecular and cortical bone by micro magnetic resonance imaging. *J Magn Reson Imaging*. 2007;25:390–409.

16. Rajapakse CS, Leonard MB, Bhagat YA, et al. Micro-MR imaging-based computational biomechanics demonstrates reduction in cortical and trabecular bone strength after renal transplantation. *Radiology*. 2012;262:912–20.
17. Wehrli FW, Hopkins JA, Hwang SN, et al. Cross-sectional study of osteopenia with quantitative MR imaging and bone densitometry. *Radiology*. 2000;217:527–38.
18. Thompson PM, Apostolova LG. Computational anatomical methods as applied to ageing and dementia. *Br J Radiol*. 2007;80(Spec No 2):S78–91.
19. Robbins S, Evans AC, Collins DL, Whitesides S. Tuning and comparing spatial normalization methods. *Med Image Anal*. 2004;8:311–23.
20. Davies RH, Twining CJ, Cootes TF, et al. A minimum description length approach to statistical shape modeling. *IEEE Trans Med Imaging*. 2002;21:525–37.
21. Gregory JS, Testi D, Stewart A, et al. A method for assessment of the shape of the proximal femur and its relationship to osteoporotic hip fracture. *Osteoporos Int*. 2004;15:5–11.
22. Gregory JS, Stewart A, Undrill PE, et al. Bone shape, structure, and density as determinants of osteoporotic hip fracture: a pilot study investigating the combination of risk factors. *Invest Radiol*. 2005;40:591–7.
23. Baker-LePain JC, Luker KR, Lynch JA, et al. Active shape modeling of the hip in the prediction of incident hip fracture. *J Bone Miner Res*. 2011;26:468–74.
24. Goodyear SR, Barr RJ, McCloskey E, et al. Can we improve the prediction of hip fracture by assessing bone structure using shape and appearance modeling? *Bone*. 2012;53:188–93.
25. Li W, Kezele I, Collins DL, et al. Voxel-based modeling and quantification of the proximal femur using inter-subject registration of quantitative CT images. *Bone*. 2007;41:888–95.
26. Li W, Kornak J, Harris T, et al. Identify fracture-critical regions inside the proximal femur using statistical parametric mapping. *Bone*. 2009;44:596–602.
27. Poole KE, Treece GM, Mayhew PM, et al. Cortical thickness mapping to identify focal osteoporosis in patients with hip fracture. *PLoS One*. 2012;7:e38466.
28. Carballido-Gamio J, Harnish R, Saeed I, et al. Geometry, density distribution and internal structure of the proximal femur in relation to age and hip fracture risk in women. Minneapolis, MN: ASBMR; 2012.
29. •• Carballido-Gamio J, Harnish R, Saeed I, et al. Proximal femoral density distribution and structure in relation to age and hip fracture risk in women. *J Bone Miner Res*. 2013;28:537–46. *Article demonstrating the spatial relationship of vBMD in the proximal femur with incident hip fracture and aging in women.*
30. Davatzikos C, Vaillant M, Resnick SM, et al. A computerized approach for morphological analysis of the corpus callosum. *J Comput Assist Tomogr*. 1996;20:88–97.
31. Johannesdottir F, Poole KE, Reeve J, et al. Distribution of cortical bone in the femoral neck and hip fracture: a prospective case-control analysis of 143 incident hip fractures: the AGES-REYKJAVIK Study. *Bone*. 2011;48:1268–76.
32. •• Poole KE, Treece GM, Ridgway GR, et al. Targeted regeneration of bone in the osteoporotic human femur. *PLoS One*. 2011;6:e16190. *Article demonstrating localized osteoporosis treatment effects on cortical bone thickness in the proximal femur.*
33. Bryan R, Nair PB, Taylor M. Use of a statistical model of the whole femur in a large scale, multi-model study of femoral neck fracture risk. *J Biomech*. 2009;42:2171–6.
34. Rueckert D, Frangi AF, Schnabel JA. Automatic construction of 3-D statistical deformation models of the brain using nonrigid registration. *IEEE Trans Med Imaging*. 2003;22:1014–25.
35. •• Nicoletta DP. Development of a parametric finite element model of the proximal femur using statistical shape and density modeling. *Comput Methods Biomech Biomed Eng*. 2012;15:101–10. *Article demonstrating the feasibility of parametric finite element modeling of the proximal femur.*
36. Keller TS. Predicting the compressive mechanical behavior of bone. *J Biomech*. 1994;27:1159–68.
37. Li W, Kornak J, Harris T, et al. Hip fracture risk estimation based on principal component analysis of QCT atlas: a preliminary study. *SPIE Med Imaging*. 2009
38. Li W, Kornak J, Harris TB, et al. Bone fracture risk estimation based on image similarity. *Bone*. 2009;45:560–7.
39. Fritscher K, Grunerbl A, Hanni M, et al. Trabecular bone analysis in CT and X-ray images of the proximal femur for the assessment of local bone quality. *IEEE Trans Med Imaging*. 2009;28:1560–75.
40. Schuler B, Fritscher KD, Kuhn V, et al. Assessment of the individual fracture risk of the proximal femur by using statistical appearance models. *Med Phys*. 2010;37:2560–71.
41. Leber S, Fritscher KD, Schmoelz W, Schubert R. Statistical model based analysis of bone mineral density of lumbar spine. *Int J Comput Assist Radiol Surg*. 2009;4:239–43.
42. Whitmarsh T, Fritscher KD, Humbert L, et al. A statistical model of shape and bone mineral density distribution of the proximal femur for fracture risk assessment. *Med Image Comput Comput Assist Interv*. 2011;14:393–400.
43. Bredbenner TL, Potter R, Mason RL, et al. Investigation of statistical shape and density modeling as a discriminator for clinical fracture risk. Toronto, CA: ASBMR; 2010. p. S83.
44. Orwoll E, Blank JB, Barrett-Connor E, et al. Design and baseline characteristics of the osteoporotic fractures in men (MrOS) study—a large observational study of the determinants of fracture in older men. *Contemp Clin Trials*. 2005;26:569–85.
45. Bredbenner TL, Mason RL, Havill LM, et al. Investigating fracture risk classifiers based on statistical shape and density modeling and the MrOS data set. San Francisco, CA: ORS; 2012.
46. Whitmarsh T, Fritscher KD, Humbert L, et al. Hip fracture discrimination from dual-energy X-ray absorptiometry by statistical model registration. *Bone*. 2012;51:896–901.
47. Carballido-Gamio J, Folkesson J, Karampinos DC, et al. Generation of an atlas of the proximal femur and its application to trabecular bone analysis. *Magn Reson Med*. 2011;66:1181–91.